Assessing the potential impacts of climate change on droughts in East Africa using CORDEX-CORE regional climate models' simulations: A focus on Tanzania

Mohamed SALAH[1,*], Fawzia MOURSY[1], Eman SOLIMAN[2], Gamil GAMAL[1,3]

[1] Natural Resources Department, Faculty of African Postgraduate Studies, Cairo University, Egypt

[2] Ministry of Water Resources and Irrigation, Giza, Egypt

[3] Department of Atmospheric Physics, Earth Science Institute, Slovak Academy of Sciences, Bratislava, Slovakia

Abstract: This study used the Standardized Precipitation Index (SPI) to detect drought episodes in Tanzania, as well as their characteristics in terms of duration (years), severity, and intensity, and analyse their trends. To conduct the analysis, 12-month standardized precipitation was employed, utilizing historical data from 1970 to 2005 and future projections from 2021 to 2100 for ten meteorological stations in Tanzania. These historical projections are based on simulations generated by Coordinated Regional Climate Downscaling Experiment (CORDEX-CORE) models. According to projected future changes, precipitation would increase at 60% of stations, notably in Tanzania's eastern regions. The highlands, however, are predicted to experience a greater rise in precipitation than the desert and semi-arid areas, which are predicted to receive less precipitation. In addition, it is expected that in the mid-future, drought events will occur more frequently in Tanzania's dry regions and will last longer and be more severe. Based on the estimated SPI values, the Mann-Kendall (MK) test and Sen's slope estimator were used to examine the drought trend. The overall analysis of the computed SPI time series demonstrated that drought is more frequent and severe in Tanzania, especially in Kigoma, Songea and Tanga. Based on the SPI-12 values, the results show that the most prolonged and severe droughts occurred during the 2039–2041, 2045–2046, 2068–2072, 2081–2083 and 2092–2095 marking extremely dry years. To mitigate the potential impacts of climate change, it is crucial to implement adaptation measures that address the specific challenges faced by Tanzania.

Key words: Tanzania, drought, climate change, SPI-index, CORDEX-CORE, precipitation

[*]corresponding author, e-mail: civil_eng_mohamedsalah@yahoo.com

doi: 10.31577/congeo.2023.53.3.6

1. Introduction

The increasing emission of greenhouse gases contributes significantly to the observed global warming (*Tan et al., 2020*), leading to escalating impacts of climate change on society and the environment (*Touma et al., 2015*). Climate change presents one of the most critical challenges for both ecosystems and human populations (*IPCC, 2013*). Without effective early adaptation measures, food and water scarcity are expected to increase under the influence of climate change (*AghaKouchak et al., 2015*). According to climate change studies, there has been an increase in climate variability in Africa, which would likely lead to more droughts (*Meze-Hausken, 2004; Thornton et al., 2014*). Drought, a natural meteorological phenomenon, refers to a prolonged period of below-normal water availability, spanning from a few days to months, and occasionally even decades (*Mukamuhirwa et al., 2020*). Its impacts are widespread, affecting various socio-economic sectors and having devastating effects on communities (*Dai, 2013; Polong et al., 2019*). Climate change and variability are expected to intensify the effects of drought in terms of complexity, frequency, and spatial extent (*Sheffield et al., 2012*). Drought can be categorized into four types: meteorological, agricultural, hydrological, and socioeconomic. The meteorological drought occurs when a specific area experiences a prolonged absence of rainfall, posing risks to agriculture and hydrology (*Wilhite and Glantz, 1985*). Recent studies suggest that distressing drought events and pluvial scenarios are expected to increase in frequency and severity in many regions (*Huang et al., 2016; Spinoni et al., 2020*). Globally, there has been a noticeable rise in drought occurrences attributed to human-induced climate change (*Masson-Delmotte et al., 2021*). Various countries in Asia (*Sahana et al., 2021*), Europe (*Stagge et al., 2017*), and America (*Sobral et al., 2019; Zhu et al., 2021*) have experienced the impacts of the drought.

At the Horn of Africa, Tanzania faces climate variability, with rainfall patterns influenced by factors like the Indian Ocean Dipole and El Niño-Southern Oscillation. Climate change is expected to worsen drought frequency and severity in these regions (*Makula and Zhou, 2022*). Human activities like deforestation, overgrazing, and land degradation can reduce land moisture retention, increasing susceptibility to droughts (*Olagunju, 2015*). Poor water resource management, including over-abstraction, inefficient irrigation systems, and inadequate storage facilities, can exacerbate water scarcity (*World Vision International, 2022*). Rapid population growth and urbanization also increase demand for water and land resources, exacerbating drought impacts (*Heidari et al., 2021; Maja and Ayano, 2021*). Drought is a recurrent natural hazard in Tanzania that has been linked to a combination of natural and human-induced factors (*Mdemu, 2021*). Additionally, *Ayugi et al. (2022)* conducted an extensive investigation into the anticipated changes in drought events specifically within the East African region. Their study revealed future projections indicating that the arid and semi-arid regions are poised to experience diminished precipitation levels and more frequent occurrences of droughts in the long term. Similarly, *Haile et al. (2020)* undertook an assessment of future drought changes across East Africa utilizing an ensemble of five Global Climate Models from the Coupled Model Intercomparison Project. Their findings suggest that the extent of drought-prone areas is likely to expand by the conclusion of the 21st century under various emission scenarios.

Researchers, policymakers, and scientists are increasingly interested in global drought monitoring and assessment. Many Methods for measuring, analysing, and characterizing drought conditions are used to advise policymakers, resource managers, and researchers in their decisions about agriculture, water resource management, and other related fields. These approaches have varying degrees of complexity and data requirements, but they all aim to comprehend and measure the severity of a drought. Metrics like Rainfall Anomaly Index (*Van Rooy, 1965*), Palmer's Drought Severity Index (*Palmer, 1968*), Standardized Precipitation Index (SPI) (*Mckee et al., 1993*), and Standardized Precipitation Evapotranspiration Index (SPEI) (*Vicente-Serrano et al., 2010*) are widely used to evaluate drought in various regions worldwide. These Common drought methods assessments include the Standardized Precipitation Index (SPI), which transforms rainfall data into standard deviations from the mean to categorize drought severity. The SPI gained popularity due to its simplicity and use of only precipitation data (*Musonda et al., 2020; Wang et al., 2022*). In applications over East Africa, studies have used the SPI to analyse trends in countries like Ethiopia, Kenya, and Tanzania (*Dutra et al., 2014; Kalisa et al., 2021*). These analyses point to increased meteorological drought associated with rising precipitation deficits, especially in recent decades. Also, climate projections estimate further increases in aridity and drought risk in the region by 2100, particularly under high emissions scenarios (*Ayugi et al., 2022*). These findings underscore the need for robust drought monitoring and assessment to support adaptation in East Africa.

Drought in Tanzania is a pressing issue that requires urgent attention and evaluation. The nation's vulnerability to drought events necessitates in-depth assessments of its potential impacts and magnitude. Understanding drought dynamics is crucial for developing effective strategies for mitigation, adaptation, and risk reduction. The main objectives of this study were (1) to evaluate the future climate of Tanzania under the Representative Concentration Pathways (RCPs), for a low-emissions scenario (RCP2.6) and a high-emissions scenario (RCP8.5), (2) to examine the temporal variation of drought in selected Tanzanian stations using high resolution CORDEX-CORE regional climate model simulations based on the Standardized Precipitation Index (SPI). (3) By quantifying the frequency and severity of these events. This study aims to better understand the risks associated with climate change and inform the development of adaptation and mitigation strategies targeted at reducing the vulnerability of communities and ecosystems to extreme weather events in the region.

2. Data and methods

2.1. Dataset

The main sources of data are Coordinated Regional Climate Downscaling Experiment (CORDEX-CORE), (*Giorgi et al., 2009*) and Coupled Model Intercomparison Project Phase 5 (CMIP5), (*Taylor et al., 2012*), which are the two major international initiatives focused on improving our understanding of climate change and its impacts. The CMIP5 models are as follows: Met Office Hadley Centre (MOHC) HadGEM2-ES model (*Collins et al., 2011*), both Max Planck Institute Earth System Models (MPI-ESM-LR and MPI-ESM-MR), (*Giorgetta et al., 2013*), and Norwegian Climate Centre, Norwegian Earth System Model version 1 (NorESM1-M) model (*Knudsen and Walsh, 2016*). The list of CORDEX climate Models presented at Table 1 and can be downloaded using the Earth System Grid Federation (*ESGF*) nodes such as `https://esgf-data.dkrz.de/`. These simulations outputs are available on CORDEX-Africa domain have spatial resolution at grid increment of $0.22° \times 0.22° (\sim 25$ km $\times$ 25 km) and temporal coverage ranging from 1970 to 2005 for historical runs and projections from 2021 to 2100. Furthermore, the Representative Concentration Pathways (RCPs), which are a set of scenarios used by climate models to project future climate change (*Moss et al., 2010*). The RCPs range from a low-emissions scenario (RCP2.6) to a high-emissions scenario (RCP8.5). They provide a standardized framework for comparing different climate scenarios and for assessing the likelihood of different outcomes (*IPCC, 2014*). We utilize the ensemble of multiple regional climate models which is a commonly used approach in climate modelling studies. This approach is often used to increase confidence in the projections by reducing the impact of any one model's biases or uncertainties (*Hawkins and Sutton, 2011; IPCC, 2013*).

Table 1. CORDEX-CORE RCM list.

Model	Institution Name	Reference
CCLM5-0-15	Climate Limited-area Modelling Community-KIT, Germany	*Rockel et al. (2008)*
REMO2015	Helmholtz-Zentrum Geesthacht, Climate Service Center, Germany	*Teichmann et al. (2013)*
RegCM4-7	Abdus Salam International Centre for Theoretical Physics	*Giorgi et al. (2012)*

2.1.1. The Standardized Precipitation Index (SPI)

For identifying, describing, and monitoring drought, the Standardized Precipitation Index (SPI) was created by (*McKee et al., 1993*). The SPI is calculated using rainfall measurements over a long period that have been adapted to a probability distribution and then transformed into a normal distribution (*Edwards and McKee, 1997*). The SPI has the following advantages: it is individually connected to probability; it can compute the recent period's precipitation deficiency; and it can monitor both wet and dry periods because it is a normalized index (*Svoboda and Fuchs, 2016*). Drought occurs once the SPI value reaches -1 or below. Oppositely, when the SPI reaches a positive number, the drought ends. The SPI index calculates precipitation insufficiency at several time intervals ranging from 1 to 48 months (*Yihdego et al., 2019*). The choice of time scale depends on the purpose of the analysis, the characteristics of the region, and the available data. The SPI-12 was chosen since it is primarily effective for identifying drought situations in dry countries like East Africa (*Haile et al., 2020*), and it was shown to be better appropriate for managing water resources (*Raziei et al., 2009*). The SPI is calculated by dividing the discrepancy between precipitation and the average during a chosen period into standard deviation, as indicated in Eq. (1).

$$SPI = \frac{x_i - \bar{x}}{\sigma_x}, \tag{1}$$

where, x_i is the observed precipitation value, $\bar{x}$ is the average of the x_i precipitation series, and the standard deviation of series σ_x. The SPI drought index threshold calculations are included in Table 2, along with their associated categories (*McKee et al., 1993; Tigkas et al., 2015*). SPI calculations are based on *DrinC* (Drought Indices Calculator) software created by the National Technical University of Athens (NTUA) (accessible at `http://drinc.ewra.net/`). DrinC has been utilized in several applications and research for drought assessment and monitoring, mostly in arid and semi-arid locations (*El-Tantawi et al., 2021; Yisehak et al., 2021*).

Table 2. Drought classification of SPI index.

Drought category	SPI Value
Extremely wet	≥ 2.0
Very wet	1.5 – 1.99
Moderately wet	1.0 – 1.49
Near normal	(-0.99) – (0.99)
Moderately dry	(-1.0) – (-1.49)
Severely dry	(-1.5) – (-1.99)
Extremely dry	≤ -2.0

2.1.2. Drought severity, intensity and duration

The degree or scope of the effects brought on by drought conditions is referred to as drought severity. It is a gauge of how severely the drought has impacted numerous environmental factors, including agriculture, water availability, ecosystems, and socioeconomic activity. The severity (S) is an aggregate summation of the index values across the length of the incident Eq. (2). Also, intensity (I), is an occurrence's severity divided by the number of dry months or years since the incident Eq. (3). The amount of time that a region is subject to drought conditions is known as the drought duration (years). It is the time frame covering the start of the drought and its end. The length of a drought is often expressed in months or years and indicates how long the area has experienced drier-than-average conditions.

$$\mathrm{S} = -\sum_{t=1}^{\mathrm{Duration}} \mathrm{SPI}_t\,, \tag{2}$$

$$\mathrm{I} = \frac{\mathrm{Severity}}{\mathrm{Duration}}\,. \tag{3}$$

2.1.3. The Mann-Kendall (MK) test

A non-parametric statistical technique called the Mann-Kendall (MK) test is used to find trends in time series data. Without making any assumptions about the distribution of the data, it is frequently used to identify whether there is a significant upward or downward trend over time in a dataset (*Yue et al., 2002*). The MK test assesses the rankings of data points in a time series to ascertain whether there is a monotonic trend over time. The Mann-Kendall test statistic is calculated according to Eq. (4):

$$\mathrm{S} = \sum_{k=1}^{n-1} \sum_{j=k+1}^{n} \mathrm{sgn}(X_j - X_k)\,, \tag{4}$$

where X_j and X_k are the data values at time j and k respectively, and $\mathrm{sgn}(X_j - X_k)$ is the sign function that returns 1 if $X_j > X_k$, -1 if $X_j < X_k$, and 0 if $X_j = X_k$.

2.1.4. The Sen's slope

The Sen's slope is a non-parametric method for estimating the slope of a linear relationship between two variables (*Sen, 1968*). It is reliable and unaffected by data outliers. Sen's slope can be positive or negative, indicating an increasing or decreasing trend. A positive slope indicates an increasing trend, while a negative slope indicates a decreasing trend. The trend is stronger the greater the absolute value of Sen's slope. Using Sen's approach, this test computes the slope and intercepts. The following formula is used to calculate a set of linear slopes Eq. (5):

$$d_k = \frac{X_j - X_i}{j - i}, \tag{5}$$

For ($1 \leq i < j \leq n$), where n is the number of data, X stands for the variable, and i, j are indices. The median of all slopes is then used to compute Sen's slope: $b = \text{Median}\{d_k\}$. Each timestep (t) intercepts are calculated according to Eq. (6):

$$a_t = X_t - b * t. \tag{6}$$

3. Target area

Tanzania, a country in East Africa, bordered by Kenya and Uganda to the north, Rwanda, Burundi, and the Democratic Republic of the Congo to the west, Zambia, Malawi, and Mozambique to the south, and the Indian Ocean to the east, with a population of around 60 million, with a majority living in rural areas (Fig. 1). The economy is primarily driven by agriculture, accounting for over 70% of employment and exports. However, recent droughts have led to food insecurity and economic hardship for rural communities (*UNDP, 2020*). Tanzania has two primary rainy seasons: unimodal (October–April) and bimodal (October–December, and March–May) (*Zorita and Tilya, 2002*). The bimodal rainfall pattern is generated by the Intertropical Convergence Zone's seasonal migration (ITCZ), which causes two distinct wet periods in the north and east of Tanzania, while other parts have only one (*NOAA, 2021*).

The historical climate of Tanzania investigated based of the Climate Research Unit (CRU) observation data through the period (1971–2020). The supplementary tables (S1, S2 and S3 – see the online Supplement) presented the monthly mean statistics of minimum and maximum temperature (°C) and precipitation (mm/day). The coldest months with minimum temperature are June and July, with mean temperatures of 15.02 °C and 14.25 °C, respectively. The warmest months are March and December, with mean temperatures of 18.46 °C and 18.52 °C, respectively. The Mann-Kendall test identifies significant positive trends in Minimum Temperature data for all months, ranging from 0.29 °C in April to 0.57 °C in November (S1). In addition, the warmest months with maximum temperature are October and March, with mean temperatures of 30.01 °C and 29.02 °C, respectively. The coolest month is July, with a mean temperature of 26.60 °C. The Mann-Kendall results show a significant increasing trend in almost all the months, whereas March and April show no statistically significant trend (S2). While for the precipitation (S3), the wet season months, January, February, March, and December, experience higher precipitation levels (3–5 mm/day), and moderate coefficients of variation (CV), indicating consistency in precipitation patterns. On the other hand, the dry season months, June, July, August, and September, experience significantly lower rainfall (0.3–0.6 mm/day), with high coefficients of variation. The standard deviation (StDev) values are higher for wet season months, reflecting larger fluctuations in rainfall amounts, while lower for dry season months, indicating more stable and consistent precipitation patterns. The Mann-Kendall test identifies no statistically significant trend precipitation trends, with increasing trends from September to March, and decreasing trends from April to July. The sensitivity slope values measure precipitation rate change, with positive sensitivity slopes for increasing trends and negative values for decreasing trends (S3).

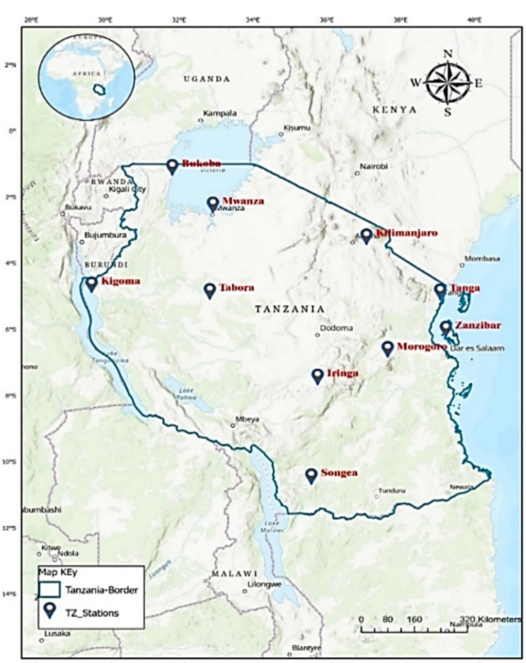

Fig. 1. Spatial distribution of the 10 meteorological stations in Tanzania area map.

4. Results and discussion

4.1. Climate change assessment for Tanzanian stations (2021–2100)

Based on the ensemble mean of the CORDEX-CORE regional climate simulations, Table 3 displays the annual mean and the MK test for the precipitation (mm) during the historical period (1970–2005) and on the future period (2021–2100) under RCP2.6 and RCP8.5 scenarios. Historically, the Mann-Kendall (MK) test results for Bukoba, Iringa, Kigoma, Kilimanjaro, Morogoro, Mwanza, Songea, Tabora, Tanga, and Zazibar show varying mean precipitation values. Bukoba has a high mean precipitation, indicating a relatively rainy location. Iringa has a lower mean precipitation compared to Bukoba, suggesting a drier climate. Kigoma has a high mean precipitation, like Bukoba, with a wide range of precipitation values. Kilimanjaro has the lowest mean precipitation, indicating a drier climate. Morogoro has moderate mean precipitation, with a moderate standard deviation. Mwanza has a moderate mean precipitation, with a moderate standard deviation. Songea has a moderate mean precipitation, with a negative MK test result suggesting a decreasing trend. Tabora has a relatively lower mean precipitation, with a low standard deviation. Tanga has a high mean precipitation, with a high standard deviation. Zanzibar has a very high mean precipitation, with a high standard deviation, indicating significant variability. The positive MK test results suggest a positive trend in precipitation, though significance should be considered.

The projected Precipitation statistics (mm) based on the period 2021–2100 for Tanzania under the RCP2.6 scenario, revealing Zanzibar with the highest mean precipitation (2005.0 mm) and Kilimanjaro with the lowest (598.0 mm), suggesting drier conditions. Zanzibar has the highest StDev value (309.7 mm), indicating greater variability in projected precipitation. The Mann-Kendall test identifies significant trends in projected precipitation data, with Kilimanjaro station showing significant positive trends, Kigoma and Mwanza showing negative trends, and the rest showing no statistically significant trends. Additionally, Table 3, displays projected Precipitation statistics (mm) for Tanzania under the RCP8.5 scenario, revealing the highest mean precipitation (1970.5 mm) in Zanzibar, followed by Kilimanjaro with the lowest mean precipitation (639.8 mm) and potentially drier conditions. Zanzibar has the highest maximum precipitation

(2744.6 mm), indicating potential for extreme rainfall events. Kilimanjaro has the lowest maximum precipitation (953.2 mm), suggesting limited rainfall even during extreme events. The minimum precipitation values represent the driest months experienced at each location. Higher StDev values indicate greater variability in projected precipitation, indicating more uncertain precipitation patterns. The Mann-Kendall results show significant positive trends in projected precipitation in Bukoba, Mwanza, Kilimanjaro, and Tabora, while Tanga has a significant negative trend. The remaining locations show no statistically significant trend in their projected precipitation patterns.

Table 3. The annual mean and the MK test of the precipitation (mm) for the historical period (1970–2005) and the projected period (2021–2100) under the RCP2.6 and RCP8.5.

Station	**Historical**		**RCP2.6**		**RCP8.5**	
	Mean (mm)	**MK test**	**Mean (mm)**	**MK test**	**Mean (mm)**	**MK test**
Bukoba	1224.2	0.01	1293.8	0.0	1372.7	0.4***
Iringa	867.4	−0.2	844.0	0.1	835.1	0.1
Kigoma	1377	−0.2	1344.6	−0.1	1325.0	−0.1
Kilimanjaro	578.5	0.04	598.3	0.2**	639.8	0.2**
Morogoro	816.6	−0.03	846.2	0.1	853.2	0.1
Mwanza	875.5	−0.01	918.2	−0.1	963.6	0.3**
Songea	966.6	−0.12	924.2	0.0	904.1	−0.1
Tabora	782	−0.14	772.6	0.1	775.7	0.2**
Tanga	1379.3	0.1	1433.9	0.1	1399.4	−0.2*
Zanzibar	1916.2	0.1	2005.0	0.1	1970.5	−0.1

Note: * – P-value < 0.05, ** – P-value < 0.01, *** – P-value < 0.001

Figure 2 shows the relative changes in precipitation (%) under two scenarios: RCP2.6 and RCP8.5 for each station. The RCP2.6 and RCP8.5 scenarios predict increased precipitation about (3–12%) in several regions, including Bukoba, Kilimanjaro, Morogoro, Mwanza, Tanga, and Zanzibar. RCP8.5 indicates a more significant increase in precipitation, suggesting a higher impact under the high emission scenario. Stations Iringa, Kigoma, Songea and Tabora experience a decrease around (1–7%). Kilimanjaro experiences a higher increase in precipitation, while Morogoro experiences a slightly larger increase. Stations Tanga and Zanzibar experience a larger increase in precipitation, suggesting a higher impact under the lower emission scenario. Generally, the expected rise in precipitation in a high emission scenario shows how anthropogenic GHG emissions have an impact. The findings of this research are consistent with earlier studies on East Africa that showed a considerable increase in precipitation under high emission scenarios compared to low forcing sustainability pathways (*Onyutha et al., 2021; Ayugi et al., 2021; 2022; Makula and Zhou 2022*).

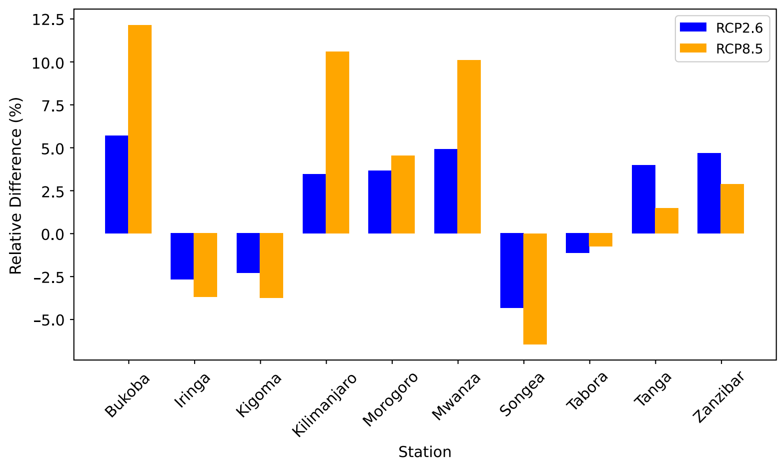

Fig. 2. The relative change of precipitation for the future period (2021–2100) under RCP2.6 and RCP8.5.

Additionally, Table S4 (online Supplement) shows projected Maximum Temperature statistics (°C) for Tanzania under the RCP2.6 and RCP8.5 scenarios. Tanga, Kigoma, and Bukoba have the highest mean maximum temperatures (30.96 °C), with higher StDev values and higher CV values. Kilimanjaro has significant negative trends in projected maximum temperature, while the rest show no statistically significant trend. Table S5 (online Supplement) presents projected Minimum Temperature statistics (°C) for selected locations in Tanzania under the RCP2.6 and RCP8.5 scenarios. Zanzibar has the highest mean minimum temperature (25.71 °C), while Iringa has the lowest (16.33 °C), suggesting potentially cooler conditions. Stations with higher StDev values exhibit greater variability in projected minimum temperatures, indicating more uncertain temperature patterns. Mwanza and Tabora have higher CV values, suggesting greater variability in projected minimum temperatures. Morogoro station shows a significant positive trend in projected minimum temperature, suggesting a potential increase in temperatures under the low emissions RCP2.6 scenario. Table S5 also shows projected Minimum Temperature statistics for selected locations under the RCP8.5 scenario. Zanzibar has the highest mean minimum temperature (26.91 °C), Iringa has the lowest (17.86 °C), and Tabora and Iringa have higher CV values, suggesting greater variability in projected minimum temperatures. The Figure 3 presents the box plot range of the maximum and minimum temperature difference for all stations under RCP2.6 and RCP8.5 emission scenarios. The projected warming will raise the minimum temperature and maximum temperature in average of 0.11–0.26 °C/decade and 0.11–0.24 °C/decade under RCP2.6 and RCP8.5, respectively. A persistent increase in mean and extreme temperature properties over East Africa in comparison to other sub-regions of the continent has been noted by recent research based on CMIP6 models (*Almazroui et al., 2020; Ayugi et al., 2021; Iyakaremye et al., 2021*). For example, according to *Almazroui et al. (2020)*, the warming trend over East Africa under different Shared Socioeconomic Pathways (SSPs) is anticipated to be 0.03, 0.22, and 0.49 °C/decade, respectively. Drought episodes are predicted to occur more frequently because of the rising temperature and decreasing precipitation over most of Africa.

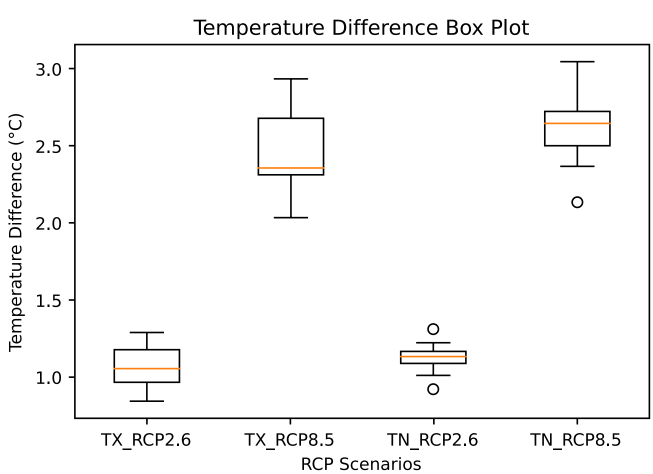

Fig. 3. The Temperature difference range for minimum and maximum temperatures for both RCP2.6 and RCP8.5 scenarios.

4.2. Drought heatmap for Tanzania

4.2.1. Tanzania historical SPI-12 (1970–2005)

The following provided dataset (Fig. S6) is a heatmap showing the standardized precipitation index (SPI-12) classification for various stations in Tanzania between 1970 and 2005. The classification scheme used in this dataset ranges from extremely dry (less than −2.00) to extremely wet (greater than or equal to 2.00), with several intermediate categories. It appears that Tanzania has experienced extreme weather conditions in the past, with instances of both extreme drought and extremely wet conditions. The years 1976–1979 experienced periods of extremely wet conditions in Kilimanjaro, Morogoro, Tanga, Mwanza, and Bukoba, while in 1998–1999 Zanzibar experienced extremely wet conditions. On the other hand, the years 1988–1989 and 2004–2005 experienced extreme drought conditions in Morogoro, Iringa, Kigoma, Songea, and Tabora.

4.2.2. Tanzania SPI-12 under RCP2.6 emission scenario (2021–2100)

Figure S7 shows Tanzania stations under RCP2.6 scenario. The dataset provides SPI-12 values for ten different stations across Tanzania for each year between 2021 and 2100. From the heatmap, it is evident that the precipitation pattern varies significantly across the different stations in Tanzania. For instance, Bukoba and Mwanza stations have relatively high SPI values, indicating wetter conditions compared to the other stations such as Iringa and Kilimanjaro, which have negative SPI values, indicating drier conditions. The heatmap for Extreme Drought shows that Tabora is expected to have the most frequent extreme drought events, with occurrences in 2039–2040, 2040–2041, and 2082–2083. Iringa is also expected to have multiple extreme drought events, with occurrences in 2031–2032, 2040–2041, and 2099–2100. In contrast, the heatmap for extremely wet shows that Kilimanjaro, Morogoro, Tanga, and Zanzibar are expected to have the most frequent occurrences of extreme wet events in 2027–2028, while Morogoro is the only station expected to have an extreme wet event in 2036–2037. The differences between these results suggest that different regions in Tanzania may experience different patterns of extreme precipitation events under the RCP2.6 scenario. For example, Tabora and Iringa are expected to experience more frequent extreme drought events, while Kilimanjaro, Morogoro, Tanga, and Zanzibar are expected to experience more frequent extreme wet events.

4.2.3. Tanzania SPI-12 under RCP8.5 emission scenario (2021–2100)

The dataset provides information about Tanzania's drought conditions at different stations between 2021 and 2100 under RCP8.5 scenario (Fig. S8). Analysing the dataset reveals that there are variations in precipitation levels across different stations and years. For instance, some stations like Zanzibar experienced extremely wet conditions in 2021–2022, while others like Iringa and Bukoba experienced dry conditions during the same period. However, Kilimanjaro station had a consistent moderate condition throughout the years. Under RCP8.5 scenario, most stations are likely to experience moderate to severe dry conditions, with some experiencing extremely dry conditions in the future. For instance, Tabora station experienced extreme drought conditions in the years 2026–2027, 2077–2078, and 2094–2095. Iringa station experienced extreme drought conditions in the years 2026–2027, and 2071–2072. Additionally, in terms of extremely wet periods, we can observe that some stations experience multiple wet periods. For example, Tanga station experiences extremely wet conditions in the years 2027–2028 and 2030–2031. Mwanza station experiences extremely wet conditions in the years 2075–2076 and 2088–2089.

As presented in the Figures S6, S7 and S8 (online Supplement), the temporal distribution of SPI-12 reveals noteworthy drought (wetness) events during the mid-future (far future) under the RCP2.6 and RCP8.5 scenarios. Furthermore, the study indicates a link between drought/flood changes and warming levels, with extreme precipitation events likely to increase in high emission scenarios. This aligns with the IPCC 2021 report, which predicts an increase in extreme wet events due to human-induced greenhouse gas emissions (*IPCC, 2021*). The persistent dry anomaly in the mid-future is evidence of drying patterns, first detected in 1999 due to sea surface temperature changes in the tropical Pacific basin (*Lyon and DeWitt, 2012*). The shift from drought to wet events in the future is attributed to increased atmospheric moisture (*Trenberth, 2011*).

4.3. Trend analysis of annual drought with SPI-12 time series

The Mann–Kendall test and Sen's slope were devoted to identifying trends of SPI-12 values in Tanzania. Table 4 shows the Mann-Kendall (MK) trend test results of the SPI-12 values for different stations in Tanzania under historical conditions and two different climate change scenarios (RCP2.6 and RCP8.5). A significant positive MK trend suggests a statistically significant increasing trend in precipitation, while a significant negative MK trend suggests a statistically significant decreasing trend in precipitation.

Table 4. Mann-Kendall (MK) trend test results of the SPI-12 values for different stations in Tanzania under historical conditions and two different climate change scenarios (RCP2.6 and RCP8.5).

Station	**MK test**			**Sen's slope**		
	Hist.	**RCP2.6**	**RCP8.5**	**Hist.**	**RCP2.6**	**RCP8.5**
Bukoba	−0.02	−0.01	0.44***	−0.003	−0.001	0.03
Iringa	−0.11	0.11	0.06	−0.01	0.01	0.004
Kigoma	−0.07	−0.09	−0.15	−0.01	−0.01	−0.01
Kilimanjaro	0.01	0.23**	0.22**	0.001	0.02	0.02
Morogoro	−0.03	0.08	0.13	−0.01	0.01	0.01
Mwanza	0.04	−0.08	0.28***	0.004	−0.01	0.02
Songea	−0.03	0.03	−0.13	−0.004	0.003	−0.01
Tabora	−0.08	0.05	0.18*	−0.01	0.004	0.01
Tanga	0.05	0.06	−0.20*	0.01	0.004	−0.01
Zanzibar	0.05	0.13	−0.1	0.01	0.008	−0.01

Note: * – P-value < 0.05, ** – P-value < 0.01, *** – P-value < 0.001

For the historical period, most locations show negative MK values, indicating periods of below-average precipitation in the past like Iringa and Bukoba. However, the MK test for the rest of stations as Kilimanjaro is generally close to zero, suggesting near-average precipitation historically. Under the RCP2.6 scenario, there is a mix of positive and negative MK test, indicating potential shifts between wetter and drier conditions compared to historical conditions. Under both scenarios, only Kilimanjaro station shows significant positive MK trends around 0.22, suggesting increasing precipitation trends. Under the RCP8.5 scenario, there are more positive MK test values, indicating more instances of above-average precipitation compared to historical conditions. Some locations show significant positive (Bukoba, Kilimanjaro and Mwanza) or negative (Tanga) MK trends, suggesting significant increasing or decreasing precipitation trends under RCP8.5.

4.4. The analysis of drought characteristics and their categories

Figure 4, presents the number of drought events for various weather stations in Tanzania for historical period and two different climate scenarios RCP2.6 and RCP8.5. The drought events are categorized into Sever Drought, Mod. Drought, Mild Drought, Mild Wet, Mode. Wet, and Sever Wet. Most stations have experienced a low frequency of severe drought events historically, with several stations reporting zero occurrences. However, Kilimanjaro and Tanga stations have consistently experienced moderate occurrences of severe drought. Several stations including Iringa, Kigoma, Kilimanjaro, Morogoro, Mwanza, and Songea, have faced moderate and mild drought events across all scenarios, indicating their vulnerability to drought conditions. Under the RCP2.6 scenario, most regions are expected to experience more "Moderate Drought" and "Mild Drought" occurrences. This implies that even under a more optimistic scenario with reduced greenhouse gas emissions, Tanzania is still likely to face challenges related to water scarcity and agricultural productivity. The RCP8.5 scenario, which represents a high greenhouse gas emission trajectory, predicts a higher number of severe drought events in several regions. Stations like Iringa, Kigoma, and Morogoro are particularly susceptible to severe drought conditions, with potential implications for water resources and agricultural activities.

4.5. Drought characteristics analysis

This study characterized and analysed drought duration (in years), severity, and intensity by utilizing SPI values generated at 12-month timescale at ten meteorological stations across Tanzania. Table 5 provides valuable insights into the longest drought incidents recorded at various meteorological stations and their categorization based on the intensity during the study period. The data reflects the historical conditions as well as projections under different climate scenarios, including RCP2.6 and RCP8.5. The results highlight the significant variability in drought occurrences across different regions in the study area. For instance, the station Bukoba experienced a moderate

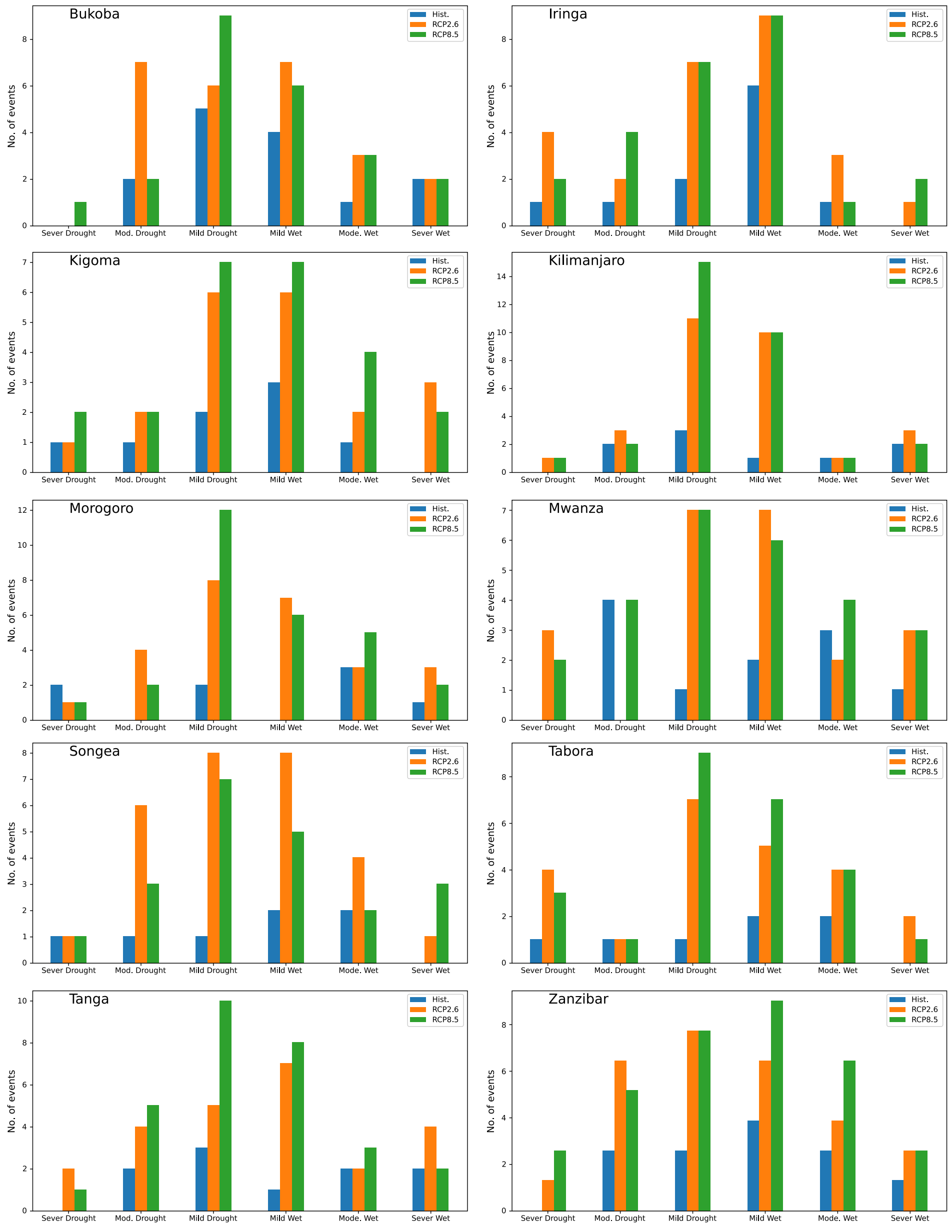

Fig. 4. The number of moderate, severe, and extreme events detected under SPI-12 for each station.

Table 5. The longest drought incidents recorded, and their categories of dryness based on the intensity during the study period for each meteorological station.

Station		**Year**	**Duration**	**Severity**	**Intensity**	**Category**
Bukoba	Hist	1973–1975 1974–1975	2	−2.78	−1.39	moderately drought
	RCP2.6	2058–2059 2059–2060	2	−2.53	−1.27	moderately drought
	RCP8.5	2040–2041 2041–2042	2	−3.57	−1.79	severely drought
Iringa	Hist	1988–1989	1	−1.57	−1.57	severely drought
	RCP2.6	2022–2023 2023–2024 2024–2025 2025–2026	4	−5.34	−1.33	moderately drought
	RCP8.5	2025–2026 2026–2027	2	−3.29	−1.65	severely drought
Kigoma	Hist	1989–1990 1990–1991 1991–1992	3	−4.09	−1.36	moderately drought
	RCP2.6	2066–2067 2067–2068	2	−3.47	−1.73	severely drought
	RCP8.5	2077–2078 2078–2079	2	−2.63	−1.31	moderately drought
Kilimanjaro	Hist	1974–1975	1	−1.36	−1.36	moderately drought
	RCP2.6	2022–2023 2023–2024 2024–2025 2025–2026 2026–2027	5	−5.66	−1.13	moderately drought
	RCP8.5	2039–2040 2040–2041 2041–2042	3	−3.79	−1.26	moderately drought

Table 5. Continued from the previous page.

Morogoro	Hist	1974–1975	1	−1.41	−1.41	moderately drought
	RCP2.6	2023–2024 2024–2025	2	−3.1	−1.5	severely drought
	RCP8.5	2022–2023 2023–2024	2	−2.25	−1.12	moderately drought
Mwanza	Hist	1988–1989	1	−1.75	−1.75	severely drought
	RCP2.6	2048–2049 2049–2050 2050–2051	3	−6.29	−2.1	extremely drought
	RCP8.5	2040–2041 2041–2042 2042–2043	3	−3.75	−1.25	moderately drought
Songea	Hist	1987–1988 1988–1989	2	−2.98	−1.49	moderately drought
	RCP2.6	2055–2056 2056–2057	2	−2.28	−1.14	moderately drought
	RCP8.5	2067–2068 2068–2069	2	−2.31	−1.16	moderately drought
Tabora	Hist	1987–1988 1988–1989	2	−3.11	−1.55	severely drought
	RCP2.6	2039–2040 2040–2041	2	−4.26	−2.13	extremely drought
	RCP8.5	2024–2025 2025–2026 2026–2027	3	−5	−1.67	severely drought
Tanga	Hist	1999–2000 2000–2001	2	−3.63	−1.81	severely drought
	RCP2.6	2029–2030 2030–2031	2	−2.09	−1.04	moderately drought
	RCP8.5	2068–2069 2069–2070	2	−3.87	−1.94	severely drought

Table 5. Continued from the previous page.

Zanzibar	Hist	1999–2000	2	−3.88	−1.94	severely drought
		2000–2001				
	RCP2.6	2029–2030	2	−2.18	−1.09	moderately drought
		2030–2031				
	RCP8.5	2068–2069	2	−2.85	−1.43	moderately drought
		2069–2070				

Note: Duration (years) – The amount of time the region experienced drought conditions, Severity – Cumulative SPI values over the drought duration period, and Intensity – Severity divided by Duration (dimensionless)

drought incident during the historical period, whereas the RCP8.5 scenario projected a severe drought incident, indicating a potential worsening of drought conditions in the future. Similarly, Iringa station recorded a severe drought incident historically, and the RCP2.6 scenario suggested a moderate drought incident, which indicates some variations in the severity and frequency of droughts. On the other hand, Mwanza station witnessed an extreme drought incident under the RCP2.6 scenario, signalling a heightened risk of prolonged and severe droughts in the region.

Generally, relative to the baseline period, most areas under the two scenarios are projected to experience drought duration (DD) in the mid-future than the far future over Tanzania (Table 5). For instance, drought duration for SPI-12 under the most scenario for mid-future shows varying patterns of drought changes at stations Bukoba, Kilimanjaro, Mwanza, Songea and Tabora likely to experience a higher number of years affected by drought as compared to other stations of the study area. The emission effect from RCP2.6 scenario on drought duration is distinct in the mid-future but not evident in the far future. Interestingly, drought duration shows a reduction in occurrence toward the far-century (2071–2100), except in the northwestern (Kigoma station), and southeastern (Songea station). Overall, the findings from various stations reveal that while some areas may experience a reduction in drought severity, others might face an increase in the frequency and intensity of drought events, especially under the RCP8.5 scenario.

As shown in Table 5, the study calculated the drought severity (DS), which is defined as the total SPI value over the course of the drought event and is used to determine the severity of the drought. The severity of the drought increases with the DS value. According to the various scenarios, Tanzania is predicted to endure a drought that is more severe in the mid- and long-term future. The large increase in DD as shown in Table 5, partially explains why DS increases substantially more in the mid-term than in the long-term. Regarding Kigoma, Mwanza, Songea, and Tabora stations, there is an intriguingly larger DS for the low emission concentration (Table 5), although in the distant future, the impacts of emission concentration on DS are less significant.

The analysis of the drought intensity (DI), which is determined by dividing the length of the drought by its severity, is shown in Table 5. The overall intensity of drought events is gauged using the DI. Under various scenarios, the mean DI values are estimated for historical and future time periods. In general, in the various scenarios, Tanzania's DI maintains similar levels or declines in the far future and rises in the mid-future relative to the baseline period. Under RCP2.6 and RCP8.5, DI is projected to have an influence on Tanzania's northeast and east in the mid-term (Table 5).

5. Measures to reduce the effects of future droughts

Climate change projections show a significant increase in droughts, particularly in East Africa and Tanzania towards the end of the 21st century and the warmer RCP 8.5 emission scenario. This could lead to recurrent droughts in most East African countries, particularly in the Horn African countries (*Osima et al., 2018*). The combined effects could negatively impact the livelihoods of people living in coastal areas, lake regions, highlands, and arid and semiarid lands of Tanzania. Climate change projections also lead to increasing aridity in East Africa, affecting key sectors such as agriculture, water, energy, and health (*Osima et al., 2018; Serdeczny et al., 2017*). Understanding projected spatiotemporal changes in future drought patterns is crucial for taking mitigation measures before the full range of projected drought risks affects societal setups and the overall environments. Mitigation measures include greater implementation of environmental rehabilitation approaches and water resources management strategies, which are essential to combat future water shortages and land degradation over East Africa (*Gebremeskel et al., 2018; Haile et al., 2019*). Efficient drought management and monitoring, designing response policies and strategies at national, regional, and international levels, are required to build resiliencies to future droughts (*Haile et al., 2019; Sheffield et al., 2014*). Building a drought-resilient economy for drought-vulnerable societies can help reduce the future impacts of droughts on socioeconomic activities and natural ecosystem functions across East Africa (*Mwangi et al., 2014; Shukla et al., 2014*).

6. Summary and conclusions

Determining the severity of a drought in a certain area requires knowledge of its characteristics. The Eastern Africa, including Tanzania has experienced drought crises often throughout the past fifty years, particularly from 1988 to 2010. Ten meteorological stations located throughout Tanzania were used in this study to assess and analyse drought characteristics such as duration (years), severity, and intensity. Additionally, the Mann–Kendall (MK) trends test combined with Sen's slope Estimator was employed to detect trends of the Standardized Precipitation Index (SPI) values. The monthly precipitation for Tanzania based on CRU dataset from 1971 to 2020 identifies no significant precipitation trends, while minimum and maximum temperature exhibit significant increasing trends in most months.

Based on CORDEX-CORE simulations, under RCP2.6 scenario, the Mann-Kendall test for precipitation reveals significant positive trend in Kilimanjaro station, while under the RCP8.5, stations Bukoba, Kilimanjaro, Mwanza and Tabora have significant positive trend in precipitation, while Tanga station examined a significant negative trend. All stations have significant positive trend of maximum and minimum temperatures under RCP8.5 scenario. Under RCP2.6 scenario, Kilimanjaro shows significant negative trends and Morogoro station shows a positive trend for maximum and minimum temperature, respectively.

From the standardized precipitation index (SPI-12) classification for Tanzania between 1970 and 2005, it is evident that the region has experienced extreme weather conditions, including extreme drought and extreme wet periods in 1976–1979, 1998–1999, and 1988–1989 and 2004–2005. From SPI-12 heatmap, under RCP2.6 scenario (2021–2100), extreme drought events are more frequent in Tabora and Iringa, while extremely wet events are more frequent in Kilimanjaro, Morogoro, Tanga, and Zanzibar under the RCP8.5

scenario. Some stations experienced extreme wet conditions, while others, like Zanzibar, experienced dry conditions. Kilimanjaro station maintained a consistent moderate condition. Most stations are expected to experience moderate to severe dry conditions, with some experiencing extremely dry conditions in the future.

The Mann-Kendall test and Sen's slope were used to identify trends in SPI-12 values in Tanzania. Most locations showed negative SPI values, suggesting below-average precipitation in the past but near-average precipitation for most stations. The RCP2.6 scenario shows mixed positive and negative SPI values, suggesting potential shifts between wetter and drier conditions. Kilimanjaro station shows positive MK trends, while RCP8.5 shows more positive SPI values and significant positive or negative MK trends in some locations.

Furthermore, The RCP2.6 scenario predicts more moderate and mild droughts in Tanzania, highlighting challenges related to water scarcity and agricultural productivity. The RCP8.5 scenario predicts more severe droughts, with Iringa, Kigoma, and Morogoro stations being particularly vulnerable. Results show significant variability in drought occurrences across regions, with some areas experiencing a reduction in severity while others may face an increase in frequency and intensity, particularly under the RCP8.5 scenario. These findings underscore the urgency of implementing climate mitigation and adaptation strategies to minimize the impacts of severe droughts in the future.

Acknowledgements. We would like to acknowledge the World Climate Research Programme (WCRP) Coupled Model Intercomparison Project (CMIP5) and CORDEX climate modelling institutes for generously providing access to their valuable model output. We thank the climate data operator (CDO) for performing some of the research analysis. Also, we appreciate the anonymous reviewers' diligent reading of our article and their informative remarks and recommendations.

Authors' contributions. All authors contributed to the study conception and design.

Declarations. All authors certify that they have no affiliations with or involvement in any organization or entity with any financial interest or non-financial interest in the subject matter or materials discussed in this manuscript.

References

AghaKouchak A., Feldman D., Hoerling M., Huxman T., Lund J., 2015: Water and climate: Recognize anthropogenic drought. Nature, **524**, 7566, 409–411, doi: 10.1038/524409a.

Almazroui M., Saeed F., Saeed S., Islam M. N., Ismail M., Klutse N. A. B., Siddiqui M. H., 2020: Projected change in temperature and precipitation over Africa from CMIP6. Earth Syst. Environ., **4**, 455–475, doi: 10.1007/s41748-020-00161-x.

Ayugi B., Dike V., Ngoma H., Babaousmail H., Mumo R., Ongoma V., 2021: Future changes in precipitation extremes over East Africa based on CMIP6 models. Water, **13**, 17, 2358, doi: 10.3390/w13172358.

Ayugi B., Shilenje Z. W., Babaousmail H., Lim Kam Sian K. T. C., Mumo R., Dike V. N., Iyakaremye V., Chehbouni A., Ongoma V., 2022: Projected changes in meteorological drought over East Africa inferred from bias-adjusted CMIP6 models. Nat. Hazards, **113**, 2, 1151–1176, doi: 10.1007/s11069-022-05341-8.

Collins W. J., Bellouin N., Doutriaux-Boucher M., Gedney N., Halloran P., Hinton T., Hughes J., Jones C. D., Joshi M., Liddicoat S., Martin G., O'Connor F., Rae J., Senior C., Sitch S., Totterdell I., Wiltshire A., Woodward S., 2011: Development and evaluation of an Earth-system model –HadGEM2. Geosci. Model Dev., **4**, 4, 1051–1075, doi: 10.5194/gmd-4-1051-2011.

Dai A., 2013: Increasing drought under global warming in observations and models. Nat. Clim. Change, **3**, 1, 52–58, doi: 10.1038/nclimate1633.

DrinC: Drought Indices Calculator http://drinc.ewra.net/.

Dutra E., Wetterhall F., Di Giuseppe F., Naumann G., Barbosa P., Vogt J., Pozzi W., Pappenberger F., 2014: Global meteorological drought – Part 1: Probabilistic monitoring. Hydrol. Earth Syst. Sci., **18**, 7, 2657–2667, doi: 10.5194/hess-18-2657-2014.

Edwards D. C., McKee T. B., 1997: Characteristics of 20th century drought in the United States at multiple time scales. Atmospheric Science Paper No. 634, Climatology Report, No. 97-2, Department of Atmospheric Sciences, Colorado State University.

El-Tantawi A. M., Bao A., Liu Y., Gamal G., 2021: Assessment of meteorological drought in North-Western Egypt using rainfall deciles, standardized precipitation index and reconnaissance drought index. Disaster Adv., **14**, 1, 1–14.

ESGF: http://esgf-data.dkrz.de/. ESGF (Earth System Grid Federation) Node at DKRZ (Deutsches Klimarechenzentrum – German Climate Computing Centre).

Gebremeskel G., Gebremicael T. G., Girmay A., 2018: Economic and environmental rehabilitation through soil and water conservation, the case of Tigray in northern Ethiopia. J. Arid Environ., **151**, 113–124, doi: 10.1016/j.jaridenv.2017.12.002.

Giorgetta M. A., Jungclaus J., Reick C. H., Legutke S., Bader J., Böttinger M., Brovkin V., Crueger T., Esch M., Fieg K., Glushak K., Gayler V., Haak H., Hollweg H.-D., Ilyina T., Kinne S., Kornblueh L., Matei D., Mauritsen T., Mikolajewicz U., Mueller W., Notz D., Pithan F., Raddatz T., Rast S., Redler R., Roeckner E., Schmidt H., Schnur R., Segschneider J., Six K. D., Stockhause M., Timmreck C., Wegner J., Widmann H., Wieners K.-H., Claussen M., Marotzke J., Stevens B., 2013: Climate and carbon cycle changes from 1850 to 2100 in MPI-ESM simulations for the Coupled Model Intercomparison Project phase 5. J. Adv. Model. Earth Syst., **5**, 3, 572–597, doi: 10.1002/jame.20038.

Giorgi F., Jones C., Asrar G., 2009: Addressing climate information needs at the regional level: the CORDEX framework. WMO Bull., **58**, 3, 175–183.

Giorgi F., Coppola E., Solmon F., Mariotti L., Sylla M. B., Bi X., Elguindi N., Diro G. T., Nair V., Giuliani G., Turuncoglu U. U., Cozzini S., Güttler I., O'Brien T. A., Tawfik A. B., Shalaby A., Zakey A. S., Steiner A. L., Stordal F., Sloan L. C. Brankovic C., 2012: RegCM4: model description and preliminary tests over multiple CORDEX domains. Clim. Res., **52**, 7–29, doi: 10.3354/cr01018.

Haile G. G., Tang Q., Sun S., Huang Z., Zhang X., Liu X., 2019: Droughts in East Africa: Causes, impacts and resilience. Earth-Sci. Rev., **193**, 146–161, doi: 10.1016/j.earscirev.2019.04.015.

Haile G. G., Tang Q., Hosseini-Moghari S.-M., Liu X., Gebremicael T. G., Leng G., Kebede A., Xu X., Yun X., 2020: Projected impacts of climate change on drought patterns over East Africa. Earth's Future, **8**, 7, e2020EF001502, doi: 10.1029/2020EF001502.

Hawkins E., Sutton R., 2011: The potential to narrow uncertainty in projections of regional precipitation change. Clim. Dyn., **37**, 1-2, 407–418, doi: 10.1007/s00382-010-0810-6.

Heidari H., Arabi M., Warziniack T., Sharvelle S., 2021: Effects of urban development patterns on municipal water shortage. Front. Water, **3**, 694817, doi: 10.3389/frwa.2021.694817.

Huang J., Yu H., Guan X., Wang G., Guo R., 2016: Accelerated dryland expansion under climate change. Nat. Clim. Chang., **6**, 166–171, doi: 10.1038/NCLIMATE2837.

IPCC, 2013: Climate Change 2013: The Physical Science Basis. Contribution of Working Group I to the Fifth Assessment Report of the Intergovernmental Panel on Climate Change [Stocker T. F., D. Qin, G.-K. Plattner, M. Tignor, S. K. Allen, J. Boschung, A. Nauels, Y. Xia, V. Bex and P.M. Midgley (Eds.)]. Cambridge University Press, Cambridge, United Kingdom and New York, NY, USA, 1535 p.

IPCC, 2014: Climate Change 2014: Impacts, Adaptation, and Vulnerability. Retrieved from https://www.ipcc.ch/report/ar5/wg2/.

IPCC, 2021: The Physical science basis. Contribution of Working Group I to the Sixth Assessment Report of the Intergovernmental Panel on Climate Change [Masson-Delmotte V., Zhai P., Pirani A., Connors S. L., Péan C., Berger S., Caud N., Chen Y., Goldfarb L., Gomis M. I., Huang M., Leitzell K., Lonnoy E., Matthews J. B. R., Maycock T. K., Waterfield T., Yelekçi O., Yu R., Zhou B. (Eds.)]. Cambridge University Press, Cambridge, United Kingdom and New York, NY, USA, 2391 p., doi: 10.1017/9781009157896.

Iyakaremye V., Zeng G., Yang X., Zhang G., Ullah I., Gahigi A., Vuguziga F., Asfaw T. G., Ayugi B., 2021: Increased high-temperature extremes and associated population exposure in Africa by the mid-21st century. Sci. Total Environ., **790**, 148162, doi: 10.1016/j.scitotenv.2021.148162.

Kalisa W., Igbawua T., Ujoh F., Aondoakaa I. S., Namugize J. N., Zhang J., 2021: Spatio-temporal variability of dry and wet conditions over East Africa from 1982 to 2015 using quantile regression model. Nat. Hazards, **106**, 3, 2047–2076, doi: 10.1007/s11069-021-04530-1.

Knudsen E. M., Walsh J. E., 2016: Northern Hemisphere storminess in the Norwegian Earth System Model (NorESM1-M). Geosci. Model Dev., **9**, 7, 2335–2355, doi: 10.5194/gmd-9-2335-2016.

Lyon B., DeWitt D. G., 2012: A recent and abrupt decline in the East African long rains. Geophys. Res. Lett., **39**, 2, L02702, doi: 10.1029/2011GL050337.

Maja M. M., Ayano S. F., 2021: The impact of population growth on natural resources and farmers' capacity to adapt to climate change in low-income countries. Earth Syst. Environ., **5**, 2, 271–283, doi: 10.1007/s41748-021-00209-6.

Makula E. K., Zhou B., 2022: Linkage of Tanzania short rain variability to sea surface temperature over the southern oceans. Front. Earth Sci., **10**, 922172, doi: 10.3389/feart.2022.922172.

Masson-Delmotte V., Zhai P., Pirani A., Connors S. L., Péan C., Berger S., Caud N., Chen Y., Goldfarb L., Gomis M. I., Huang M., Leitzell K., Lonnoy E., Matthews J. B. R., Maycock T. K., Waterfield T., Yelekçi O., Yu R., Zhou B. (Eds.), 2021: Climate change 2021: The physical science basis. Contribution of working group I to the sixth assessment report of the intergovernmental panel on climate change, 2.

McKee T. B., Doesken N. J., Kleist J., 1993: The relationship of drought frequency and duration to time scales. Eighth Conference on Applied Climatology, American Meteorological Society, Anaheim, CA, 17–22 January, 179–184.

Mdemu M. V., 2021: Community's Vulnerability to Drought-Driven Water Scarcity and Food Insecurity in Central and Northern Semi-arid Areas of Tanzania. Front. Clim., **3**, 737655, doi: 10.3389/fclim.2021.737655.

Meze-Hausken E., 2004: Contrasting climate variability and meteorological drought with perceived drought and climate change in northern Ethiopia. Clim. Res., **27**, 1, 19–31.

Moss R. H., Edmonds J. A., Hibbard K. A., Manning M. R., Rose S. K., Van Vuuren D. P., Carter T. R., Emori S., Kainuma M., Kram T., Meehl G. A., Mitchell J. F. B., Nakicenovic N., Riahi K., Smith S. J., Stouffer R. J., Thomson A. M., Weyant J. P., Wilbanks T. J., 2010: The next generation of scenarios for climate change research and assessment. Nature, **463**, 7282, 747–756, doi: 10.1038/nature08823.

Mukamuhirwa A.; Hovmalm H. P.; Ortiz R.; Nyamangyoku O., Prieto-Linde M. L.; Ekholm A., Johansson E., 2020: Effect of intermittent drought on grain yield and quality of rice (*Oryza sativa* L.) grown in Rwanda. J. Agron. Crop Sci., **206**, 2, 252–262, doi: 10.1111/jac.12380.

Musonda B., Jing Y., Iyakaremye V., Ojara M., 2020: Analysis of Long-Term Variations of Drought Characteristics Using Standardized Precipitation Index over Zambia. Atmosphere, **11**, 12, 1268, doi: 10.3390/atmos11121268.

Mwangi E., Wetterhall F., Dutra E., Di Giuseppe F., Pappenberger F., 2014: Forecasting droughts in East Africa. Hydrol. Earth Syst. Sci., **18**, 2, 611–620, doi: 10.5194/hess-18-611-2014.

NOAA, 2021: The National Centers for Environmental Information (NOAA). Accessible at: `http://ncdc.noaa.gov/`.

Olagunju T. E., 2015: Impacts of human-induced deforestation, forest degradation and fragmentation on food security. N. Y. Sci. J., **8**, 1, 4–16.

Onyutha C., Asiimwe A., Ayugi B., Ngoma H., Ongoma V., Tabari H., 2021: Observed and future precipitation and evapotranspiration in water management zones of Uganda: CMIP6 projections. Atmosphere, **12**, 7, 887, doi: 10.3390/atmos12070887.

Osima S. E., Indasi V. S., Zaroug M. A. H., Edris H. S., Gudoshava M., Misiani H. O., Nimusiima A., Anyah R. O., Otieno G., Ogwang B. A., Jain S., Kondowe A. L., Mwangi E., Lennard C., Nikulin G., Dosio A., 2018: Projected climate over the Greater Horn of Africa under 1.5 °C and 2 °C global warming. Environ. Res. Lett., **13**, 6, 065004, doi: 10.1088/1748-9326/aaba1b.

Palmer W. C., 1968: Keeping Track of Crop Moisture Conditions, Nationwide: The New Crop Moisture Index. Weatherwise, **21**, 4, 156–161, doi: 10.1080/00431672.1968.9932814.

Polong F., Chen H., Sun S., Ongoma V., 2019: Temporal and spatial evolution of the standard precipitation evapotranspiration index (SPEI) in the Tana River basin, Kenya. Theor. Appl. Climatol., **138**, 1-2, 777–792, doi: 10.1007/s00704-019-02858-0.

Raziei T., Saghafian B., Paulo A. A., Pereira L. S., Bordi I., 2009: Spatial patterns and temporal variability of drought in western Iran. Water Resour. Manag., **23**, 3, 439–455, doi: 10.1007/s11269-008-9282-4.

Rockel B., Will A., Hense A., 2008: The regional climate model COSMO-CLM (CCLM). Meteorologische Zeitschrift, **17**, 4, 347–348, doi: 10.1127/0941-2948/2008/0309.

Sahana V., Mondal A., Sreekumar P., 2021: Drought vulnerability and risk assessment in India: Sensitivity analysis and comparison of aggregation techniques. J. Environ. Manage., **299**, 113689, doi: 10.1016/j.jenvman.2021.113689.

Sen P. K., 1968: Estimates of the regression coefficient based on Kendall's Tau. J. Am. Stat. Assoc., **63**, 324, 1379–1389, doi: 10.2307/2285891.

Serdeczny O., Adams S., Baarsch F., Coumou D., Robinson A., Hare W., Schaeffer M., Perrette M., Reinhardt J., 2017: Climate change impacts in Sub-Saharan Africa: From physical changes to their social repercussions. Reg. Environ. Change, **17**, 6, 1585–1600, doi: 10.1007/s10113-015-0910-2.

Sheffield J., Woo E. F., Roderick M. L., 2012: Little change in global drought over the past 60 years. Nature, **491**, 7424, 435–438, doi: 10.1038/nature11575.

Sheffield J., Wood E. F., Chaney N., Guan K., Sadri S., Yuan X., Olang L., Amani A., Ali A., Demuth S., Ogallo L., 2014: A drought monitoring and forecasting system for sub-Sahara African water resources and food security. Bull. Am. Meteorol. Soc., **95**, 6, 861–882, doi: 10.1175/BAMS-D-12-00124.1.

Shukla S., McNally A., Husak G., Funk C., 2014: A seasonal agricultural drought forecast system for food-insecure regions of East Africa. Hydrol. Earth Syst. Sci., **18**, 10, 3907–3921, doi: 10.5194/hess-18-3907-2014.

Sobral B. S., de Oliveira-Júnior J. F., de Gois G., Pereira-Júnior E. R., de Bodas Terassi P. M., Muniz-Júnior J. G. R., Lyra G. B., Zeri M., 2019: Drought characterization for the state of Rio de Janeiro based on the annual SPI index: trends, statistical tests and its relation with ENSO. Atmos. Res., **220**, 141–154, doi: 10.1016/j.atmosres.2019.01.003.

Spinoni J., Barbosa P., Bucchignani E., Cassano J., Cavazos T., Christensen J. H., Christensen O. B., Coppola E., Evans J., Geyer B., Giorgi F., Hadjinicolaou P., Jacob D., Katzfey J., Koenigk T., Laprise R., Lennard C. J., Kurnaz M. L., Li D., Llopart M., McCormic N., Naumann G., Nikilun G., Ozturk T., Panitz H.-J., da Rocha R. P., Rockel B., Solman S. A., Syktus J., Tangang F., Teichmann C., Vautard R., Vogt J. V., Winger K., Zittis G., Dosio A., 2020: Future global meteorological drought hotspots: A study based on CORDEX data. J. Clim., **33**, 9, 3635–3661, doi: 10.1175/JCLI-D-19-0084.1.

Stagge J. H., Kingston D. G., Tallaksen L. M., Hannah D. M., 2017: Observed drought indices show increasing divergence across Europe. Sci. Rep., **7**, 14045, doi: 10.1038/s41598-017-14283-2.

Svoboda M., Fuchs B. A., 2016: Handbook of Drought Indicators and Indices. World Meteorological Organization (WMO) and Global Water Partnership (GWP), Integrated Drought Management Programme (IDMP), Integrated Drought Management Tools and Guidelines Series 2. Geneva, Switzerland.

Tan G., Ayugi B., Ngoma H., Ongoma V., 2020: Projections of future meteorological drought events under representative concentration pathways (RCPs) of CMIP5 over Kenya, East Africa. Atmos. Res., **246**, 105112, doi: 10.1016/j.atmosres.2020.105112.

Taylor K. E., Stouffer R. J., Meehl G. A., 2012: An overview of CMIP5 and the experiment design. Bull. Am. Meteorol. Soc., **93**, 4, 485–498, doi: 10.1175/BAMS-D-11-00094.1.

Teichmann C., Eggert B., Elizalde A., Haensler A., Jacob D., Kumar P., Moseley C., Pfeifer S., Rechid D., Remedio A. R., Ries H., Petersen J., Preuschmann S., Raub T., Saeed F., Sieck K., Weber T., 2013: How does a regional climate model modify the projected climate change signal of the driving GCM: A study over different CORDEX regions using REMO. Atmosphere, **4**, 2, 214–236, doi: 10.3390/atmos4020214.

Thornton P. K., Ericksen P. J., Herrero M., Challinor A. J., 2014: Climate variability and vulnerability to climate change: a review. Glob. Change Biol., **20**, 11, 3313–3328, doi: 10.1111/gcb.12581.

Tigkas D., Vangelis H., Tsakiris G., 2015: DrinC: a software for drought analysis based on drought indices. Earth Sci. Inform., **8**, 3, 697–709, doi: 10.1007/s12145-014-0178-y.

Touma D., Ashfaq M., Nayak M. A., Kao S.-C., Diffenbaugh N. S., 2015: A multi-model and multi-index evaluation of drought characteristics in the 21st century. J. Hydrol., **526**, 196–207, doi: 10.1016/j.jhydrol.2014.12.011.

Trenberth K. E., 2011: Changes in precipitation with climate change. Clim. Res., **47**, 1-2, 123–138, doi: 10.3354/cr00953.

UNDP (United Nations Development Programme), 2020: Human Development Report 2020: The Next Frontier: Human Development and the Anthropocene. New York.

Van Rooy M. P., 1965: A Rainfall Anomaly Index Independent of Time and Space. Notos, **14**, 43–48.

Vicente-Serrano S. M., Beguería S., López-Moreno J. I., 2010: A Multiscalar Drought Index Sensitive to Global Warming: The Standardized Precipitation Evapotranspiration Index. J. Clim., **23**, 7, 1696–1718, doi: 10.1175/2009JCLI2909.1.

Wang Q., Zhang R., Qi J., Zeng J., Wu J., Shui W., Wu X., Li J., 2022: An improved daily standardized precipitation index dataset for mainland China from 1961 to 2018. Sci. Data, **9**, 124, doi: 10.1038/s41597-022-01201-z.

Wilhite D. A., Glantz M. H., 1985: Understanding: the drought phenomenon: the role of definitions. Water Int., **10**, 3, 111–120, doi: 10.1080/02508068508686328.

World Vision International, 2022: available online (accessed on September 21st 2023): https://www.wvi.org/stories/tanzania/solving-water-challenge-tanzania-our-commitment-most-vulnerable.

Yihdego Y., Vaheddoost B., Al-Weshah R. A., 2019: Drought indices and indicators revisited. Arab. J. Geosci., **12**, 3, 69, doi: 10.1007/s12517-019-4237-z.

Yisehak B., Shiferaw H., Abrha H., Gebremedhin A., Hagos H., Adhana K., Bezabh T., 2021: Spatio-temporal characteristics of meteorological drought under changing climate in semi-arid region of northern Ethiopia. Environ. Syst. Res., **10**, 21, doi: 10.1186/s40068-021-00226-4.

Yue S., Pilon P., Cavadias G., 2002: Power of the Mann–Kendall and Spearman's rho tests for detecting monotonic trends in hydrological series. J. Hydrol., **259**, 1-4, 254–271, doi: 10.1016/S0022-1694(01)00594-7.

Zhu Y., Liu Y., Wang W., Singh V. P., Ren L., 2021: A global perspective on the probability of propagation of drought: From meteorological to soil moisture. J. Hydrol., **603A**, 126907, doi: 10.1016/j.jhydrol.2021.126907.

Zorita E., Tilya F. F., 2002: Rainfall variability in Northern Tanzania in the March-May season (long rains) and its links to large-scale climate forcing. Clim. Res., **20**, 1, 31–40, doi: 10.3354/cr020031.